Phase boundary of θ phase of solid oxygen in ultrahigh magnetic fields

T. Nomura,* Y. H. Matsuda,† S. Takeyama, A. Matsuo, and K. Kindo
Institute for Solid State Physics, University of Tokyo, 5-1-5 Kashiwa, Chiba 277-8581, Japan

T. C. Kobayashi
Department of Physics, Okayama University, Okayama 700-8530, Japan
(Received 15 May 2015; published 13 August 2015)

The phase diagram of solid oxygen in the magnetic-field-temperature (B-T) plane is revealed by magnetization and magnetotransmission measurements. The high-field phase of solid oxygen, which we term the θ phase, is induced at the temperature below 42 K. The transition fields at the α-θ and β-θ transitions are almost temperature independent, with the phase boundary being very steep. This phase boundary indicates that the entropy change is very small at the α-θ and β-θ transitions, in contrast to the entropy-driven β-γ transition at zero field. We argue that the θ phase differs from the high-temperature γ phase in terms of entropy; the molecular rotation is inhibited in the θ phase, whereas permitted in the γ phase. This finding consolidates the novelty of the θ phase.

DOI: 10.1103/PhysRevB.92.064109 PACS number(s): 75.30.Kz, 75.50.Ee, 75.50.Xx

I. INTRODUCTION

Among all molecular crystals, solid oxygen exhibits unique properties because of the magnetic nature of molecular oxygen O_2, which has spin quantum number $S = 1$. Below the melting temperature 54.4 K, oxygen molecules form a cubic structure, called the γ phase [1]. The γ phase is characterized by paramagnetism and plasticity that is caused by molecular rotation to achieve large entropy S. Thus, the γ phase corresponds to the intermediate solid state in which the molecules are translationally ordered while orientationally disordered. At 43.8 K, the molecular axis is fixed in one direction, and the rhombohedral β phase appears [1]. In the β phase, O_2 molecules form a triangular lattice in the basal plane, where the geometrical frustration suppresses the antiferromagnetic long-range order. At 23.9 K, the geometrical frustration is lifted by the lattice deformation in the basal plane, and the monoclinic α phase is induced [1]. The α phase is known to be the only antiferromagnetic insulator consisting of a single chemical species [2].

In solid oxygen, the exchange interaction between O_2 molecules makes a significant contribution to the condensation energy as well as the van der Waals interaction. This competition leads to a strong interplay between magnetic, structural, and molecular orientational degrees of freedom. For instance, in the β-α transition, the crystal structure of solid oxygen is deformed by the magnetic ordering. The coupling between the magnetic and structural systems suggests that the external magnetic field affects the crystal structure of solid oxygen or even gives rise to a phase transition.

Recently, we have found a novel phase of solid oxygen by applying a magnetic field as high as 120 T [3]. Here, we call it the θ phase, an eighth phase of solid oxygen [4–9]. The observed α-θ phase transition is understood by the microscopic rearrangement in the O_2-O_2 dimer [3]. The O_2-O_2 dimer alignment is expected to change from rectangular parallel to canted or crossed geometries (H $\rightarrow$ S or X-type geometries) through the application of high magnetic fields because the latter geometries could result in ferromagnetic exchange couplings [10,11]. This molecular rearrangement could lead to a new packing structure of solid oxygen which is unstable at zero field. So far, the θ phase is suggested to have a cubic structure and large magnetic susceptibility [3]. However, the relation between the θ and other phases (α, β, and γ) is still unclear. For further understanding, the phase diagram needs to be clarified in the magnetic-field-temperature (B-T) plane. The phase diagram provides the thermodynamic characteristics of each phase and will clarify the property of the θ phase.

In this paper, we report the B-T phase diagram of solid oxygen determined by magnetization and magnetotransmission measurements. For the phase diagram, the sweep-speed dependence of the transition fields is taken into account. The thermodynamic property of the θ phase is discussed by focusing on the α-θ and β-θ phase boundaries. Finally, the θ phase is shown to differ from the γ phase in terms of entropy and to have an orientationally ordered packing structure that differs from that of other phases of solid oxygen.

II. EXPERIMENT

Magnetic fields are generated up to 205 T with a duration time of 6–8 μs using the single-turn coil system at the Institute for Solid State Physics, University of Tokyo [12]. Temperature is controlled from 4 to 42 K by using a liquid-He flow cryostat. For the magnetization measurement, an inductive method using a parallel twin-type pickup coil is employed [13]. For the measurement of the magnetotransmission spectra, a high-speed streak camera and a xenon arc flash lamp are employed [14]. In both measurements, the sample space is exchanged with high-purity O_2 gas and cooled to the condensation temperature. See the Supplemental Material [15] for details of the experimental procedure.

III. RESULTS

Magnetization (M) and the time derivative (dM/dt) curves of the α and β phases are shown in Figs. 1(a) and 1(b),

*t.nomura@issp.u-tokyo.ac.jp
†ymatsuda@issp.u-tokyo.ac.jp

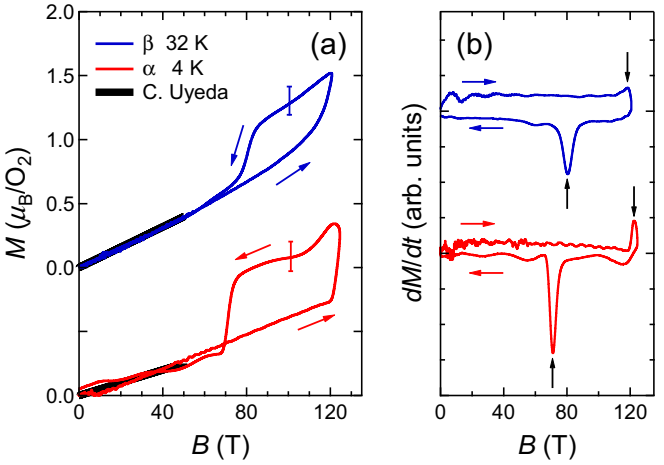

FIG. 1. (Color online) (a) Magnetization and (b) the dM/dt curves of solid oxygen. $B_{\mathrm{Max}} = 124$ T, $T = 4$ K for α phase, and $B_{\mathrm{Max}} = 121$ T, $T = 32$ K for β phase. The results of Uyeda *et al.* [16] are shown by black lines for comparison. The transition fields are determined by the dM/dt peaks, as shown by the black arrows.

respectively. The maximum fields B_{Max} and temperatures are 124 T and 4 K for the α phase and 121 T and 32 K for the β phase. Previously reported magnetization curves using a nondestructive pulse magnet [16] are shown by the black solid lines for comparison. Rapid increases in the magnetization are observed near the top of the field for both magnetization curves, indicating that the α-θ and β-θ transitions barely occur. The unsaturated values of the magnetization (compared to $M_{\mathrm{s}} = 2\mu_{\mathrm{B}}/\mathrm{O}_2$) indicate that the phase transitions are still on the way to the θ phase in these fields and the sweep speed ranges [3].

Next, we show the results of the magnetotransmission measurement on the β-θ phase transition. Figure 2(a) shows the magnetic field dependence of the transmission spectra in the two-dimensional color mapping under the conditions of $B_{\mathrm{Max}} = 141$ T and $T = 32.5$ K. At a transition field around 130 T, the transmission intensity I/I_0, where I and I_0 denote the transmitted and incident light intensities, respectively, increases at all photon energy ranges, just like in the α-θ transition [3]. This change in the transmission intensity is considered to be due to the removal of the crystalline anisotropy, which causes light scattering at the domain boundaries and decreases the transmitted light. Therefore, the β-θ transition can also be judged by the rapid change of the light transmission intensity owing to the structural transformation from the rhombohedral β phase to the cubic θ phase. In this study, the transmission intensity at 2.08 or 1.93 eV is used for the analysis because no optical transition exists at these photon energies [3,17,18]. Figure 2(b) shows the representative data of the transmission at different temperatures in a magnetic field of up to $B_{\mathrm{Max}} = 143 \pm 3$ T. Corresponding time derivatives of the transmission are shown in Fig. 2(c). The transmission intensities are normalized so that the difference from minimum to maximum is unity. The rapid increases in the transmission near the top of the field indicate that the α-θ and β-θ transitions occur. These results are consistent with the magnetization curves shown in Fig. 1.

IV. SWEEP-SPEED DEPENDENCE OF THE TRANSITION FIELDS

Prior to the construction of the phase diagram, the sweep-speed dependence of the transition field is evaluated. As indicated in a previous study [3], the α-θ transition is of first order, and the transition field depends on the sweep speed of the pulsed magnetic field. To obtain a reliable phase boundary, a slower sweep speed is favored (ideally, the quasistatic condition). In this study, the transition fields (B_{c}^{+} in up sweeps and B_{c}^{-} in down sweeps) are defined by the peak positions

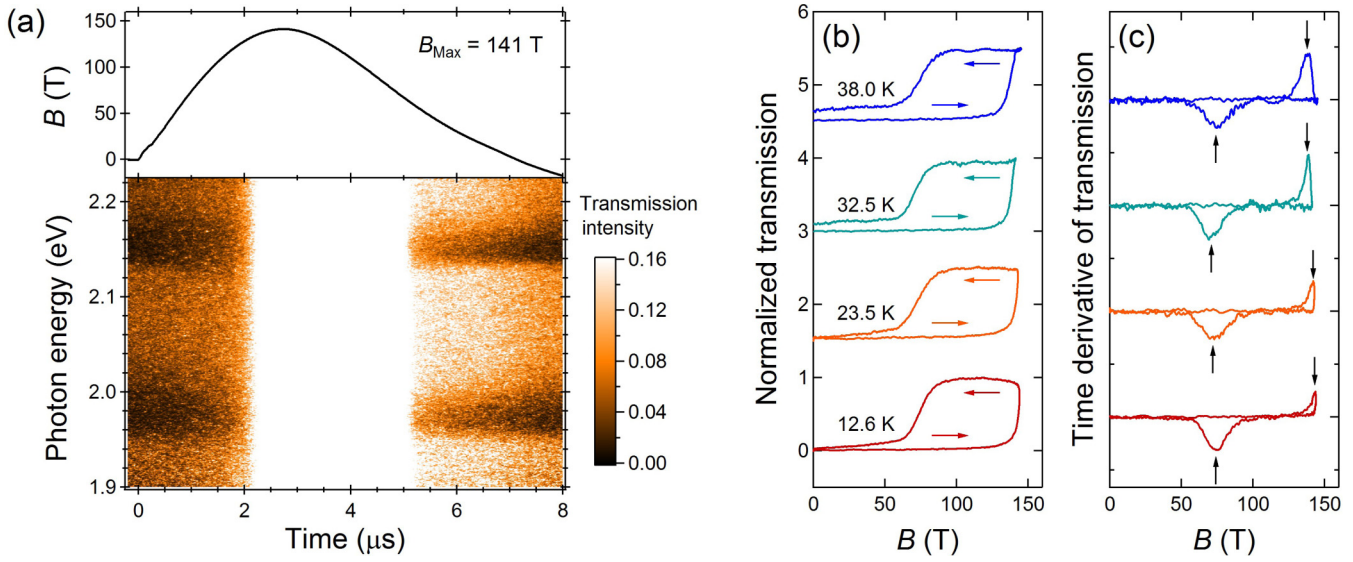

FIG. 2. (Color online) (a) Magnetic field dependence of the transmission spectra of the β phase in a two-dimensional color mapping under the conditions of $B_{\mathrm{Max}} = 141$ T and $T = 32.5$ K. (b) Normalized light transmission intensities and (c) their time derivatives of solid oxygen at the temperatures of 12.6, 23.5, 32.5, and 38.0 K. The maximum field strengths are 143 ± 3 T for all curves. The transition fields are determined by peaks of the time-derivative signal, as shown by the black arrows.

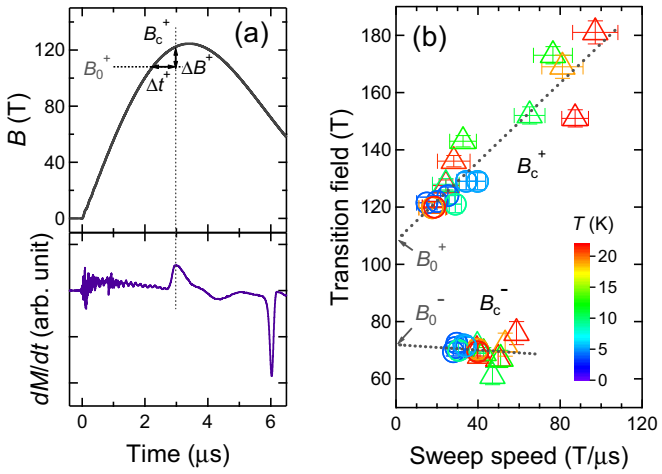

FIG. 3. (Color online) (a) Schematic definition of the sweep speed in up sweep, $\Delta B^+/\Delta t^+$. (b) The sweep-speed dependence of the transition field (B_c^+, B_c^-). The circles are from the magnetization measurement, and the triangles are from the magnetotransmission measurement. Dotted lines show the linear fits of B_c^+ and B_c^-. All plots are the results of the α phase, and the temperatures of each plot are denoted by a color scale. The reference fields (B_0^+, B_0^-) are determined to coincide with the intercepts of the fitting lines.

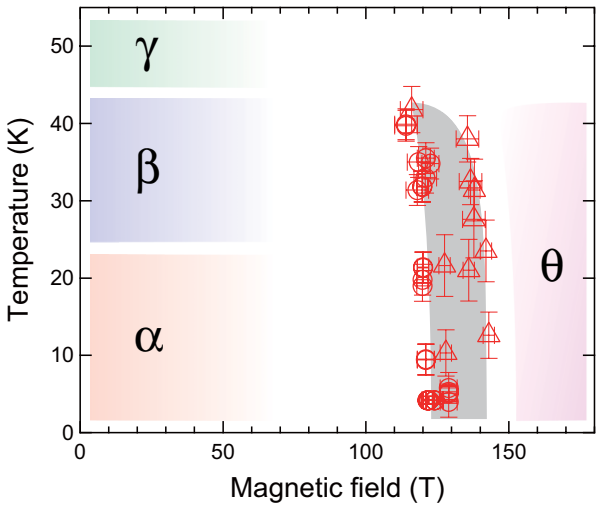

FIG. 4. (Color online) Proposed high-field phase diagram of solid oxygen for up sweep of the magnetic field. The circles are obtained from the magnetization, and the triangles are from the magnetotransmission measurement.

of the time derivatives of magnetization and transmission [Figs. 1(b) and 2(c), black arrows].

In the pulsed magnetic field, the sweep speed changes continuously. In this study, linearly averaged values are employed. Figure 3(a) shows the definition of the sweep speed with an example of the magnetization measurement in up sweep. Here, a reference field $B_0^+ = 108$ T is set to define the sweep speed around this field. The linearly averaged sweep speed from the reference field is obtained with $\Delta B^+/\Delta t^+$. The same procedure is applied for down sweep.

Figure 3(b) shows the plots of the sweep-speed dependence of the transition fields. The circles are obtained from the magnetization measurement, and the triangles are from the magnetotransmission. To minimize the effect of the temperature difference, only the data of the α phase below 22 K are plotted. The temperatures of each plot are shown in a color scale. The transition fields seem insensitive to the temperature difference in this temperature range of the α phase. Thus, all the plots are treated in the same manner in this evaluation. Dotted lines are the results of the linear fitting of B_c^+ and B_c^-. Here, the intercepts of the fitting lines correspond to the transition fields at quasistatic conditions. If the reference field B_0^+ coincides with the intercept, the deduced sweep speed is regarded as the sweep speed around the thermodynamical transition field. The reference fields (B_0^+, B_0^-) were obtained so that the above-mentioned condition was satisfied in a self-consistent way. Finally, $B_0^+ = 108$ T and $B_0^- = 72$ T are obtained, as shown in Fig. 3(b).

Here, we discuss the sweep-speed dependence of the transition fields in Fig. 3(b). As the sweep speed increases, B_c^+ increases linearly. On the other hand, B_c^- seems less sensitive to the sweep speed. In general, the transition field of the first-order transition depends on the sweep speed. The observed sweep-speed independence of B_c^- seems to be uncommon. A reliable explanation of this phenomenon is unclear at present. Therefore, in this paper, only B_c^+ is taken into account when discussing the phase diagram and the thermodynamical property of the θ phase.

V. DISCUSSION OF THE PHASE DIAGRAM

Based on the procedure stated above, the B-T phase diagram for up sweep is constructed in Fig. 4. To minimize the effect of sweep speed, only the transition fields obtained with a speed of 15–40 T/μs are employed. The transition fields B_c^+ are plotted as circles (magnetization) and triangles (magnetotransmission). The phase boundary is shown by the shaded region. The slope of the phase boundary is estimated as $|dT_c/dB_c^+| > 2$ K/T for the α-θ boundary.

The slope of the obtained phase boundary is evaluated by the magnetic Clausius-Clapeyron equation,

$$dT_c/dB_c = -\Delta M/\Delta S. \quad (1)$$

dT_c/dB_c shows the slope of the phase boundary, and ΔM and ΔS are the variations of the magnetization and entropy at the phase transition, respectively. The steep phase boundary implies that the entropy change is small. For the α-θ transition, the experiment shows that the magnetization jump $\Delta M \sim 1\mu_B = 5.6$ J T^{-1} mol^{-1} [3]. With $|dT_c/dB_c^+| > 2$ K/T, the entropy change is estimated as $|\Delta S| < 2.8$ J K^{-1} mol^{-1} $= 0.34R$, where R is the gas constant. For the β-θ transition, the result is obtained in the same order.

Here, we compare the observed ΔS with that of the temperature-induced β-γ phase transition for a quantitative argument. In the γ phase, the molecular rotation is permitted, whereas it is prohibited in the β phase. This difference gives rise to a large entropy change at the β-γ phase transition that is as high as $\Delta S_{\beta\gamma} = 2.04R$ [1,19]. This entropy change is substantially large compared with that obtained for the α-θ and β-θ transitions. Therefore, the θ phase is clearly distinguished from the γ phase with regard to the entropy. The small entropy changes in the α-θ and β-θ transitions also suggest that the molecular rotation in the θ phase is prohibited like the α and

β phases. This is a natural conclusion because the entropy of the θ phase should become zero at $T = 0$ K, as required by the third law of thermodynamics.

The phase boundary between the γ phase and the θ phase is not clear at present, although the differences between the two phases are convincing. We have not succeeded in obtaining distinct experimental evidence of the field-induced phase transition from the γ phase. We speculate that the phase boundary is rather flat and difficult to detect with the experiment with pulsed magnetic fields. Further studies with more sensitive means will be required to clarify the phase boundary of the γ phase.

If the molecular axis is ordered in the θ phase, parallel molecular packing structures (H-geometry-like) seen in other phases of solid oxygen (α, β, δ, ϵ, ζ, and η) [1,4–8] would not be realized. As expected from the O_2-O_2 dimer case [3,10,11], we currently envisage that the θ phase takes a canted molecular packing structure that locally has S or X geometries [3]. The crystal structure satisfying this condition is not very special. We think that the crystal structure of dry ice ($Pa\bar{3}$) is a candidate. This structure is known to be stable for low-temperature phases of solid CO_2, N_2, and N_2O [20].

Last, we note that the phase boundaries for α-β and β-γ are not found in our results. This seems to be strange because the α-β and β-γ transition temperatures are expected to decrease in the magnetic field because of the different susceptibilities [16,21]. This may be due to the nearly flat phase boundary, at which the phase transition gradually occurs without sharp anomalies. For the flat phase boundary, T scan is more favored than B scan.

VI. CONCLUSION

In conclusion, we have revealed the high-field phase diagram of solid oxygen in the B-T plane. The θ phase is induced not only from the α phase but also from the β phase at temperatures between 4 and 42 K. Based on the obtained α-θ and β-θ phase boundaries, the entropy changes in these transitions are found to be considerably smaller than that in the β-γ transition. We argue that in the θ phase, the molecular rotation is prohibited like the α and β phases to account for the small ΔS at the α-θ and β-θ phase transitions. This finding proves that the high-magnetic-field θ phase is different from the high-temperature γ phase, although both phases have cubic structure. There are no other cubic phases in solid oxygen. Therefore, it is concluded that a novel molecular arrangement is realized in the high-magnetic-field θ phase.

ACKNOWLEDGMENT

T.N. was supported by the Japan Society for the Promotion of Science through the Program for Leading Graduate Schools (MERIT).

[1] Yu. A. Freiman and H. J. Jodl, Phys. Rep. **401**, 1 (2004).
[2] R. Bhandari and L. M. Falicov, J. Phys. C **6**, 479 (1973).
[3] T. Nomura, Y. H. Matsuda, S. Takeyama, A. Matsuo, K. Kindo, J. L. Her, and T. C. Kobayashi, Phys. Rev. Lett. **112**, 247201 (2014).
[4] S. Klotz, Th. Strässle, A. L. Cornelius, J. Philippe, and Th. Hansen, Phys. Rev. Lett. **104**, 115501 (2010).
[5] H. Fujihisa, Y. Akahama, H. Kawamura, Y. Ohishi, O. Shimomura, H. Yamawaki, M. Sakashita, Y. Gotoh, S. Takeya, and K. Honda, Phys. Rev. Lett. **97**, 085503 (2006).
[6] L. S. Lundegaard, G. Weck, M. I. McMahon, S. Desgreniers, and P. Loubeyre, Nature (London) **443**, 201 (2006).
[7] K. Shimizu, K. Suhara, M. Ikumo, M. I. Eremets, and K. Amaya, Nature (London) **393**, 767 (1998).
[8] M. Santoro, E. Gregoryanz, H. K. Mao, and R. J. Hemley, Phys. Rev. Lett. **93**, 265701 (2004).
[9] H. Katzke and P. Tolèdano, Phys. Rev. B **79**, 140101 (2009).
[10] B. Bussery and P. E. S. Wormer, J. Chem. Phys. **99**, 1230 (1993).
[11] K. Nozawa, N. Shima, and K. Makoshi, J. Phys. Soc. Jpn. **71**, 377 (2002).
[12] N. Miura, T. Osada, and S. Takeyama, J. Low Temp. Phys. **133**, 139 (2003).
[13] S. Takeyama, R. Sakakura, Y. H. Matsuda, A. Miyata, and M. Tokunaga, J. Phys. Soc. Jpn. **81**, 014702 (2012).
[14] T. Nomura, Y. H. Matsuda, J. L. Her, S. Takeyama, A. Matsuo, K. Kindo, and T. C. Kobayashi, J. Low Temp. Phys. **170**, 372 (2013).
[15] See Supplemental Material at http://link.aps.org/supplemental/10.1103/PhysRevB.92.064109 for the experimental details and discussion.
[16] C. Uyeda, K. Sugiyama, and M. Date, J. Phys. Soc. Jpn. **54**, 1107 (1985).
[17] Yu. G. Litvinenko, V. V. Eremenko, and T. I. Garber, Phys. Status Solidi B **30**, 49 (1968).
[18] Y. B. Gaididei, V. M. Loktev, A. F. Prikhotko, and L. I. Shanskii, Phys. Status Solidi B **73**, 415 (1976).
[19] C.-H. Fagestroem and A. C. Hollis Hallett, J. Low Temp. Phys. **1**, 3 (1969).
[20] V. G. Manzhelii and Yu. A. Freiman, *Physics of Cryocrystals*, translated by M. L. Klein and A. A. Maradudin (AIP, New York, 1997).
[21] A. P. J. Jansen and A. van der Avoird, J. Chem. Phys **86**, 3597 (1987).